Mining, Metallurgy & Exploration (2021) 38:1383–1394
https://doi.org/10.1007/s42461-021-00416-9

Automated Discontinuity Extraction Software Versus Manual Virtual Discontinuity Mapping: Performance Evaluation in Rock Mass Characterization and Rockfall Hazard Identification

Juan J. Monsalve[1] · Alex Pfreundschuh[1] · Aman Soni[1] · Nino Ripepi[1]

Received: 24 September 2020 / Accepted: 11 March 2021 / Published online: 19 March 2021

Abstract
Ground control failures are one of the main causes of accidents in the underground stone mining industry. Some of the fundamental tools for rockfall hazard identification are related to rock mass characterization and geotechnical discontinuity mapping. Recent technological advances in these methods are related to remote sensing techniques and point cloud processing software for automated discontinuity mapping. Remote sensing techniques, such as LiDAR and photogrammetry, generate multi-million point clouds with millimetric precision, capturing the structure of the rock mass. The automated point cloud processing tools offer alternative algorithm-based methods to characterize and map these discontinuities. However, their applicability is constrained by multiple factors such as site specific conditions of the rock mass and the parameters used within the mapping algorithms. This paper evaluates the performance of automated discontinuity extraction software compared with manual virtual discontinuity mapping. Sampling windows from laser-scanned sections in an underground limestone mine are defined and mapped using discontinuity set extractor (DSE). Results from the virtual discontinuity software are compared with manually extracted fractures from I-Site based on reviewing orientation, trace length, spacing, number of extracted discontinuities, and processing time. The analysis determined that the automated mapping algorithm was able to identify the same discontinuity sets that had been manually mapped. The automated mapping software mapped an excessive amount of smaller fractures, which caused the comparison of both mapping techniques to be unsuccessful in terms of trace length and spacing.

Keywords Virtual discontinuity mapping · Automated discontinuity mapping · Rock mass characterization · Hazard identification · Rockfall · Underground

1 Introduction

Geomechanical failure is still one of the main causes of accidents in underground stone mines in the USA, causing 11% of the accidents in 2019 [1]. In 2011, the National Institute for Occupational Safety and Health issued the Pillar and Roof Span Design guidelines for Underground Stone mines. This document was the product of more than 10 years of research in 34 underground stone operations in the Eastern and Midwestern USA [2]. However, as it is stated in the report "… The guidelines for pillar and roof span design are empirically based; their validity, therefore, is restricted to rock conditions, mining dimensions, and pillar stresses that are similar to those included in this study…." Therefore, general methodologies that allow each mining operator to characterize and take into account site-specific conditions are required to complement existing guidelines. Moreover, these general approaches should be based on hazard identification and should allow one to evaluate the probability of rock fall, failure, or collapse [3]. These types of approaches would allow one to move on to risk assessment-based design practices [4].

Rock mass characterization is the process through which information is collected about the structure of a rock mass, the nature of its discontinuities, and the rock types that compose it [5]. This information is usually used to perform engineering analyses using analytical or numerical methods to validate the stability of an excavation or identify potential hazards within a defined rock mass [6–9]. Technological advances in discrete fracture networks (DFNs) have enabled the generation of explicit virtual 3-dimensional representations of discontinuities mapped on the field. This has yielded engineering analyses

✉ Juan J. Monsalve
jjmv94@vt.edu

[1] Mining and Minerals Engineering Department, Virginia Polytechnic Institute & State University, Blacksburg, VA, USA

that help to reduce a project's uncertainty by considering stochastic simulations [10]. However, an adequate volume of data should be collected to generate significant DFN models. Unfortunately, manual conventional rock mass characterization on occasions can be dangerous, difficult to perform, take considerable amounts of time, and provide only limited amounts of data to perform statistically sound analyses [11].

In the past 10 years, laser scanning and photogrammetry technologies have been implemented in underground excavations to perform rock mass characterization and discontinuity mapping. Researchers have proved that rock mass characterization can be performed accurately from point clouds obtained from these two methods, yielding results that agree with observations and analyses obtained through manual rock mass characterization [12, 13]. Along with these remote sensing techniques, a series of processing software and algorithms have been developed to aid engineers during the discontinuity mapping process from point clouds. Different authors have developed a series of automated and semi-automated algorithms for discontinuity mapping, either from point clouds [14, 15] or triangular irregular networks [16–19]. However, most of the case studies where these automated discontinuity extraction (ADE) algorithms are applied seem to have very well-defined discontinuities and may not represent challenging conditions that could result in other sites.

The goal of this work is to evaluate and compare discontinuity mapping results from an open-source automated discontinuity extraction software (ADES) with manual virtual discontinuity mapping (MVDM) software through the comparison of orientation, trace length, spacing, number of extracted discontinuities, and processing times. The initial section of this work describes the different software and algorithms that were used to compare both mapping methods. The following section describes the methodology used in this work which includes (1) laser scanning and scan referencing, (2) mapping windows selection, (3) virtual discontinuity mapping, (4) DSE automated mapping, (5) data processing, and 6) data analysis. Finally, results obtained from this comparison are presented and a series of conclusions are made.

2 Software

This section briefly describes the three main software that were used during the comparison process. I-Site studio was used during the MVDM process, whereas DSE and Cloud Compare were used for the ADE operation.

2.1 I-Site Studio

I-Site studio is a point cloud processing and geotechnical analysis software developed by Maptek that allows users to process and inspect multi-million-point clouds. Through the use of this software, engineers have the ability to conduct geotechnical mapping studies. The software itself contains a variety of geotechnical tools in order to formulate representative data for structural rock mass classification. The query strike and dip tool within the software allows engineers to map discontinuities by defining discontinuity planes. These planes are generated by selecting a group of points that belong to the exposed fracture on the rock face. Planes are fit by averaging the coordinates of the selected points within each individual fracture, as shown in Fig. 1. Discontinuity elements contain information such as the X, Y, Z coordinates of the element centroid, strike, dip, dip direction, maximum length, and area of the fitted plane [20].

In addition to this, once a discontinuity set has been defined, the discontinuity spacing tool can be used to measure the spacing between fractures belonging to the same set. This tool measures the shortest distance from the centroid of a discontinuity to the intersection of its normal with the projected plane of its neighboring discontinuity. Figure 2 shows a lateral view of a section where the spacing between discontinuities belonging to the same family has been measured, indicated as yellow lines. The table below this image indicates the results from this measurement, including the discontinuities used for each spacing measurement, the centroid of the initial plane, and the length of the spacing.

2.2 DSE

Discontinuity set extractor (DSE) is a MATLAB-based software developed by researchers at the Universidad de Alicante in Spain that uses a series of algorithms to automatically identify discontinuity sets from point clouds [14]. This software integrates a series of algorithms that yield point clouds containing those coplanar points that represent each defined discontinuity set. This process starts with a local curvature calculation that encompasses a nearest neighbor search and a coplanarity test that determines whether each point and its neighbors share the same plane equation. In addition to this, a normal vector to the plane is defined for each point [14].

The first step is local a curvature calculation which incorporates three distinct subsections: nearest neighbor searching (knnsearch), coplanarity test, and plan adjustments/calculation of the normal vector. The nearest neighbor method involves defining a plane of best fit within a defined range of neighboring points relative to a raw data point. Within MATLAB, the knnsearch function utilizes an algorithm that finds and calculates the nearest neighbors based on the knn search function and Euclidean distance. The function allows the user to select the nearest neighbors (k) relative to each individual point in the imported point cloud. At this point, the coplanarity of the point set must be analyzed. The coplanarity test checks every point and its associated neighbors to determine if the plane is coplanar, but if not, the plane subset will be rejected.

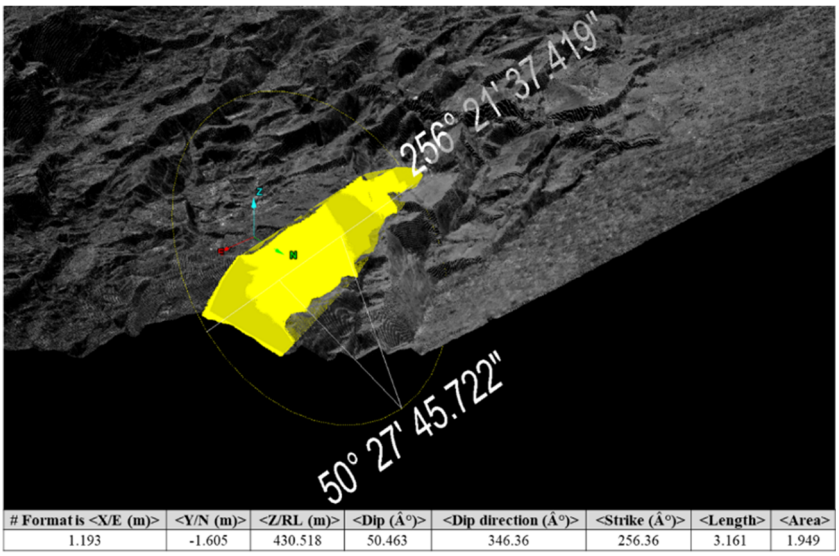

# Format is <X/E (m)>	<Y/N (m)>	<Z/RL (m)>	<Dip (Â°)>	<Dip direction (Â°)>	<Strike (Â°)>	<Length>	<Area>
1.193	-1.605	430.518	50.463	346.36	256.36	3.161	1.949

Fig. 1 I-Site discontinuity mapping and results

The test itself is derived from the principal component analysis (PCA). Following the coplanarity test, the orientation of previously identified set is computed. This process is done by identifying a normal or Eigen vector which depicts the orientation parameters of the best fit plane. From this point, the orientation of the points and their nearest neighbors are calculated to obtain a more accurate orientation [14].

The second step is the statistical analysis of the principle poles which incorporates kernel density estimation (KDE) and semi-automatic set identification. This methodology is tuned toward the parallelism of the normal vectors generated in the previous step. Statistical analysis of this methodology is conducted by the stereographic projection of the poles with respect to their planes. This is done in order to define the discontinuity sets within the point cloud of interest. The process consists of converting the plane specific normal vector and pole densities into a stereographic projection. Within DSE, the kde2d Gaussian kernel MATLAB function is used to calculate the kernel widths and pole densities. The semi-automatic set identification portion of the statistical analysis of the principle poles essentially distributes a primary "principle" orientation to every point within the point cloud. If a point's orientation differs significantly with all the principal poles, this point is not considered [14].

The final step is a cluster analysis of the data. The cluster analysis consists of clustering (DBSCAN), plane generation

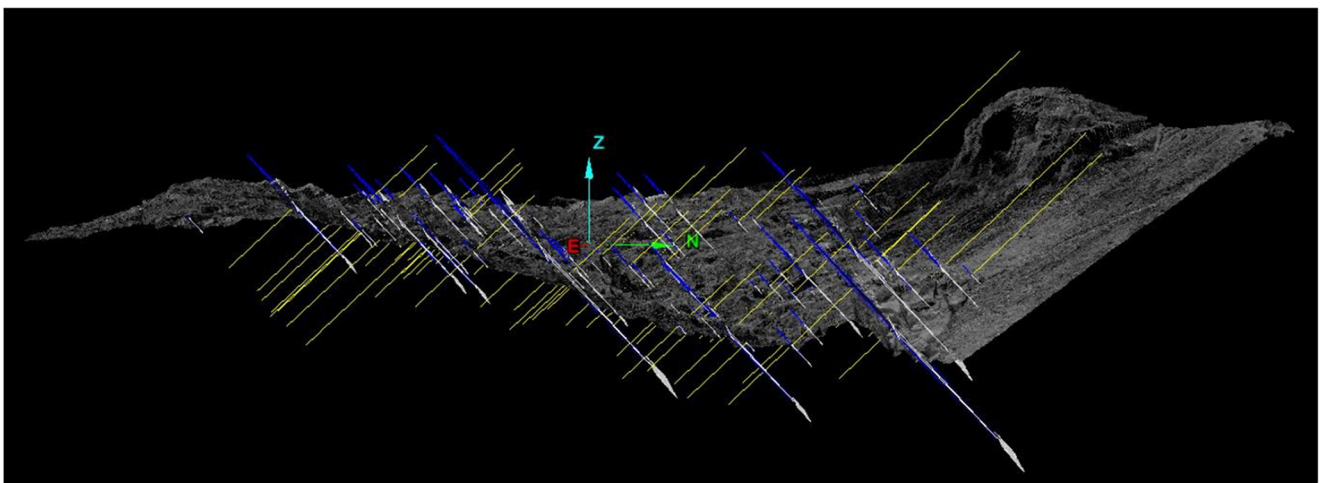

# Format is <Name>	<Length (m)>	<Centroid X Coordinate (m)>	<Centroid Y Coordinate (m)>	<Centroid Z Coordinate (m)>
discontinuity 14 to discontinuity 22	1.499	7.503	13.102	428.055
discontinuity 18 to discontinuity 22	1.323	5.942	12.188	428.349
discontinuity 21 to discontinuity 22	1.308	6.137	13.204	427.363
discontinuity 19 to discontinuity 22	1.28	5.325	12.107	428.198
discontinuity 5 to discontinuity 22	1.269	7.807	13.43	427.65

Fig. 2 I-Site discontinuity spacing measurements and results

(PCA), and an error fitting check (tolerance). The clustering process is performed by using the "density-based scan algorithm with noise" (DBSCAN) which is optimal for processing high-density, homogeneous, point clouds. The DBSCAN algorithm utilizes a series of input parameters such as the number of points to be considered within the nearest neighbor region in order to define and output clusters of points that relate to the defined principal poles. Once this is defined, plane generation takes places which takes the points attributed to a discontinuity set and cluster and defines the best fit plane algebraically. The plane is then checked to determine the quality of data fitting. The fitting check relies on a minimum module value and low standard deviation. The result from the DSE processing is a set of point clouds each individually representing the defined discontinuity sets for each mapping window analyzed [14].

2.3 Cloud Compare—Facets

Cloud Compare is an open-source point cloud processing software that has been used in different applications such as volume calculations, measuring deformations, and discontinuity mapping [15, 21–23]. Cloud Compare contains a series of plugins to perform different point cloud analyses for multiple applications. Among these plugins, FACETS is a plugin used in structural geology to map discontinuities from 3D point clouds. This plugin clusters points within a point cloud based upon user-defined coplanarity criterion. Cloud Compare was used to visualize and process point clouds generated from DSE. Using FACETS, the discontinuity set point clouds from DSE were converted into planes that were comparable to the discontinuity planes mapped in I-Site.

There are two FACET methods utilized within Cloud Compare (Kd-Tree and Fast-Marching), both utilizing a least square fitting algorithm. Clustering is computed in three different steps. The first is elementary which results in small defined planes. The second incorporates the clustering of the elementary planes that share the same coplanarity into larger planes. Finally, planes that are parallel to each other are joined into similar plane sets. Resulting planes can be exported into a CSV file type containing information about the facets such as geospatial coordinates, normal vector coordinates, dip, dip direction, horizontal and vertical extent, and surface area. The Kd-Tree algorithm divides a 3D point cloud into quarter cells until each independent cell contains points that represent a best-fit plane. This is dependent on the user input root-mean-square threshold, otherwise known as the maximum allotted distance between points. The Fast-Marching algorithm uses a lattice subdivision as defined by the octree structure. Cells that are adjacent to one another merge if the current cells' RMS value does not exceed the maximum distance criteria [15].

3 Case Study Mine

The case study mine operates in a limestone bed located in the limb of a regional syncline structure. The ore body is 100 ft thick and dips 30° toward the SE. In a previous study, the authors of the paper determined that there were four main discontinuity sets in an area adjacent of where the scans were taken for this particular study. The identified discontinuity sets were classified as follows: set 4, which corresponds to the bedding planes and contacts between rock units, which are almost parallel to the tunnel orientation and has a mean dip of 29° toward the SE; set 1, which is nearly perpendicular to the tunnel orientation and presents a subvertical dip; and sets 2 and 3, which are oblique joints with a steep dip [7]. The rock mass was defined as jointy since it presented at least 3 clear discontinuity sets throughout the excavations. In addition, radial fractures associated to the blasting were observed close to the blasthole marks in the field and in the laser scans. An average GSI of 75 was determined throughout field observations which indicates that the rock mass is a blocky. Furthermore, the main failure mechanism observed in the operation was classified as structurally controlled rock fall induced by gravity.

4 Methodology

A methodology to evaluate the performance of DSE as an ADES was proposed. This methodology compares automated mapping results obtained using DSE with those obtained using MVDM on a predefined section of the case study mine. The proposed methodology is comprised of six stages: (1) laser scanning and scan referencing, (2) mapping window selection, (3) manual virtual discontinuity mapping, (4) DSE automated mapping, (5) data processing, and (6) data analysis. This methodology can also be used to test other automated discontinuity mapping algorithm to verify their performance.

4.1 Laser Scanning and Scan Referencing

Through the utilization of a Faro Focus 3D Laser Scanner, three different scans were conducted in a defined section of the case study underground limestone mine. These scans, which ultimately result in multi-million point clouds, were downloaded from the LiDAR scanner and individually processed within Maptek's I-Site studio software. The scanned point clouds were then referenced with each other through the use of inflatable balls as reference targets, ultimately resulting in a complete referenced scan of the area of interest. The dataset was used for a geotechnical rock mass characterization and discontinuity mapping analysis for predicting and determining the potential rock fall hazards that exist. Figure 3

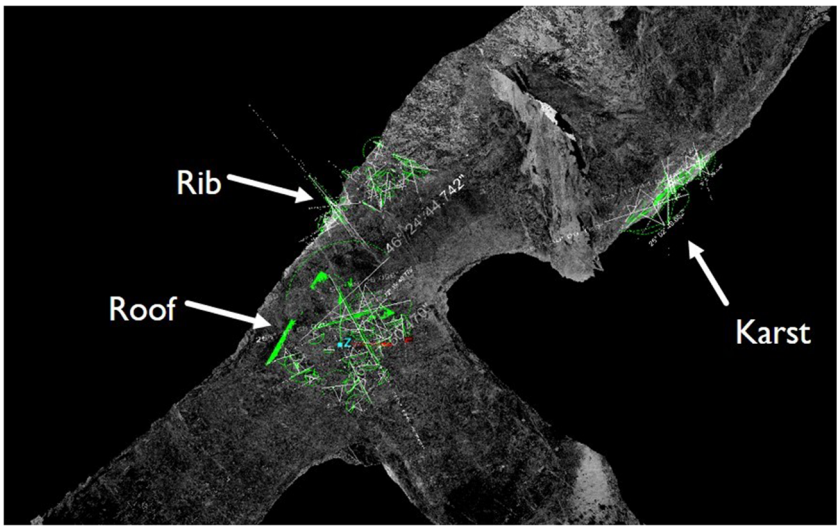

Fig. 3 Case study mine—section of interest referenced point cloud indicating mapping windows

depicts the complete referenced composite point cloud from the three separate scans of the case study section.

In order to generate the reference point cloud of the area of interest, proper registration of the different scans had to be conducted. This was imperative to avoid any errors greater than 5 mm. This process was done in I-Site by using a combination of automated initial positioning and global registration. Automated initial positioning registers scan against a predetermined reference scan by using an automated positioning method. This process provides a relatively good fit between point clouds that are registered together but must be fully registered using the global registration function. Global registration, however, aligns the pre-positioned point clouds by matching individual points and point sets in regions that contain overlap. The resulting point cloud of the section was then ready to be analyzed and sectioned off into mapping windows that display notable and uniform discontinuity planes and sets for the purpose of this analysis.

4.2 Mapping Window Selection

In order to investigate the discontinuities and resulting joint sets in the mine section, three unique mapping windows were selected within the control area. The three individual windows were from the roof, rib, and karst laden pillar areas, respectively. These windows that encompass a 12 m × 12 m area were selected based on their defined discontinuities observed both in the field and within the generated laser scanned point clouds. The areas of concern cumulatively contain approximately 11.4 million points which reduced processing time within the manual virtual and automated discontinuity mapping software as compared with the 125,939,262-points mine section point cloud. The mapping windows selected for this investigation are shown in Fig. 3.

4.3 Manual Virtual Discontinuity Mapping

Within I-Site, manual virtual discontinuity mapping was conducted. Utilizing the "Query Strike and Dip" function, the discontinuities were mapped on each of the three mapping window sections as seen below in Fig. 4.

Each discontinuity was individually identified, analyzed, and mapped for each window, and classified into discontinuity sets. Mapping these discontinuities required a high attention to detail in order to reduce the amount of points that may reside outside the plane of interest and skew the resulting averaged plane. This process is critical and should be performed by a qualified engineer or geologist not only with experience on discontinuity mapping but also field experience on the particular site.

4.4 DSE Automated Mapping

The three different mapping windows were imported into DSE in order to automatically map the discontinuities and resulting discontinuity sets that may be present. In order to calculate and cluster the points within each respective point cloud the number of nearest neighbor points had to be defined. For the purpose of this research, the input parameter for the nearest neighbors was set to 30. The nearest neighbor search was based on the point amounts rather than distance for a more accurate result. These conditions were defined by following previous recommendations by Riquelme et al. [14]. Furthermore, the number of principal poles for the algorithm to find within the sections was set to 5. This was determined based on the observation and previous knowledge of 3 to 4 joint sets that were field mapped in the mine section. The DSE MATLAB algorithm was then executed and the result was a series of five point clouds that each individually represented the clustered discontinuities associated with each of the five main principal poles for each mapping window. Clusters that

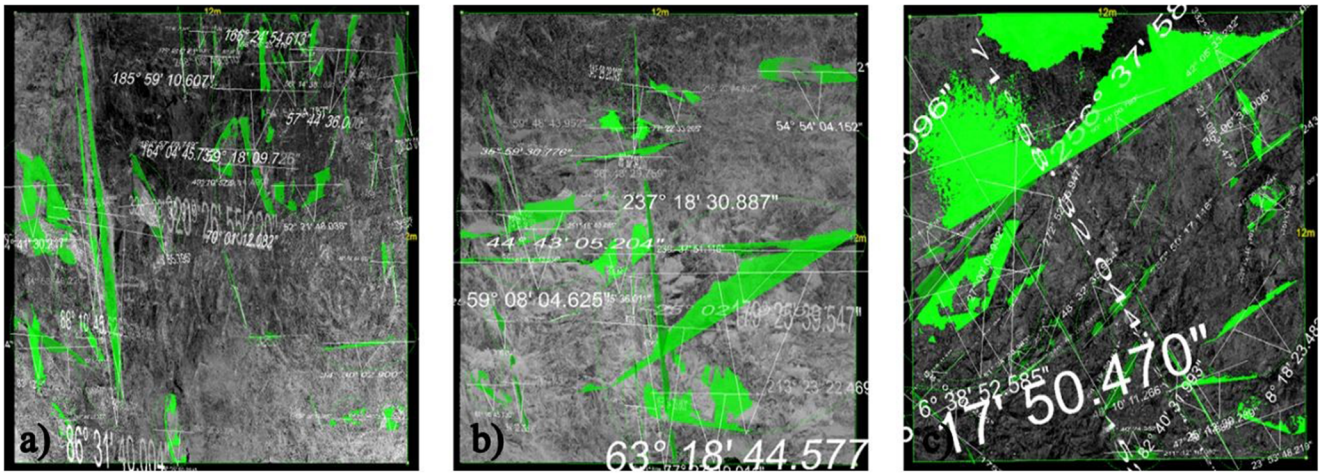

Fig. 4 I-Site mapped discontinuities. **a** Rib section. **b** Karst section. **c** Roof section

had less than 100 points were eliminated within DSE to simplify the point cloud and remove unnecessary data.

5 Data Processing

The clusters of points for the identified fracture sets were then visually examined and filtered. The physical filtering of the data to best match the observed discontinuities was conducted in Cloud Compare. The filtering of the data consisted of removing discontinuities from small sizes, along with removing surfaces that were oriented similar to discontinuities due to the structure and fracturing of the selected area. Cloud Compare was then used to generate clustered discontinuity set point clouds into facets. The two algorithms for facet generation were tested on the resulting point clouds. Facets generated from the Fast-Marching algorithm produced planes that best matched the surfaces encompassed by the points, whereas the Kd-tree method tended to partition individual discontinuities into multiple facets. Due to this, the Fast-Marching algorithm for facet generation was used. From this point, the facets for each discontinuity set within each sampling window were compared with the discontinuities mapped in I-Site.

5.1 Data Analysis

Once the discontinuities were mapped both manually with I-Site and automatically with DSE, the data analysis processes proceeded. On this stage, five main parameters were considered to evaluate the performance of the two mapping methods: processing time, number of extracted discontinuities, orientation, trace length and spacing. The processing time was evaluated based on a comparison between the time it took to map each mapping window with the time it took DSE to process each point cloud. In order to analyze the remaining parameters, four steps took place: (1) stereographic analysis and discontinuity sets definition, (2) dataset filtering, (3) probability density functions (PDFs) fitting, and (4) PDF comparison.

The stereographic analysis process was performed in the DIPS software developed by Rocscience [24]. A complied database was loaded into the software comprised of information such as x, y, and z coordinate of the centroid of each discontinuity element, dip, dip direction, and strike, length and area of the mapped plane, mapping window, and mapping software. This database was comprised of 330 discontinuity elements where 244 were mapped in DSE and 86 were mapped on I-Site. The main discontinuity sets were defined as the areas with greater pole concentrations. After each discontinuity set was defined, a new parameter was created which indicated the discontinuity set to which each fracture belonged. Those discontinuities that did not belong to any discontinuity set were not taken into account for the following steps and were considered as random fractures.

The main dataset was subsampled into six datasets filtered by mapping method and discontinuity set. Each subset was then imported into I-Site to measure the spacing between discontinuities belonging to each set and extracted from each mapping method, as previously explained in Fig. 2. At this point, there were two datasets for each subset: one containing information about the discontinuity size and the other containing information about spacing, totaling 12 datasets.

The statistical analysis software RStudio was used to perform statistical analyses on the resulting datasets by using the fitdistrplus package. PDFs were fitted and validated for discontinuity size and spacing for each dataset. The probability density functions were fitted using the maximum likelihood estimate (MLE) approach. Furthermore, the best fitting PDF was selected by comparing different models' Bayesian information criteria (BIC). The model with the lowest BIC was defined as the best fit for each parameter [25]. Spacing and trace length of manually mapped discontinuity were used as

reference dataset to compare those of the automatically extracted discontinuities using DSE.

For each joint set, the PDF of the trace lengths extracted with DSE were compared to the PDFs obtained for the same parameter for the discontinuities mapped manually on I-Site. The comparison between both distribution functions was performed by comparing the means and the standard deviation through hypothesis testing. A Student's t test was performed to evaluate if the mean trace length value of the DSE extracted data set was significantly different to the mean trace length of the reference data set. In this case, the null hypothesis was that the mean trace length for both datasets was the same. Additionally, an F test was performed between the two samples to evaluate the difference between variances of both PDFs. The hypothesis test for the F test stated that the variance for both compared datasets was the same. Both the t and F statistics calculated from these tests are associated with a p value. A p value indicates the probability for the analyzed variable to be greater than the obtained statistic. A significance value is then defined as rejection threshold value. In this case, a significance value of 0.05 was considered for both the t test and the F test. When the p value is less than the defined significance level (p value < 0.05), the null hypothesis is rejected. In the context of this study, this rejection for both the F and t tests implies that the discontinuities mapped using ADES were not the same as the manually mapped discontinuities. These two tests are only applicable if the fitted PDFs are both normal. If the fitted PDF is log-normal, this procedure can be applied as long as both data sets are normalized. The same procedure was performed to compare discontinuity spacing between the manually mapped and automatically extracted discontinuities. Figure 5 summarizes the four described steps comparing orientation, size, and spacing between discontinuities.

6 Results and Discussion

The stereographic analysis presented in Fig. 6 displays the I-Site mapped discontinuities with red crosses; the DSE extracted discontinuities with white diamonds; and a set of discontinuities that were manually mapped on the field on an area corresponding to the rib mapping window is also plotted and indicated with green triangles. Almost all discontinuities tend to cluster on three main areas. DSE extracted 244 discontinuities, whereas only 86 discontinuities were mapped from I-Site. The manually mapped discontinuities concentrate well on the areas where most of the DSE and I-Site extracted discontinuities are clustered.

Figure 7 separates DSE and I-Site extracted discontinuities in two different stereo-nets. Each pole is also scaled by discontinuity trace length, as shown in the scale under each graph. In both cases, it is possible to notice that poles are concentrating in three main areas of the stereographic net, indicating that the discontinuity orientations obtained from both methods were similar. With regard to the discontinuity trace length, it is possible to observe that both dataset scales differ. In general, DSE-extracted discontinuities have smaller lengths compared to the ones extracted from I-Site. The lower bin of the DSE extracted fractures range from 0.17 to 1.85 m and contain 193 mapped elements. Whereas the lower bin on the manually mapped discontinuities range from 0.77 to 2.60 m and are comprised of 51 fractures. This indicates that ADES tended to map smaller discontinuities, which during the manual mapping were not considered as a potential hazard for rock fall.

Results from the stereographic analysis yielded three main discontinuity sets, as shown in Fig. 8. Set 1 corresponds to the bedding plane dipping 27°, with a dip direction of 132° and a Fisher K of 118. The second set represents an oblique dipping joint dipping 47° toward 342° and a Fisher K of 24. Finally, the third discontinuity set represents a vertical parallel to the bedding dip joint, with a dip of 83° and a dip direction of 261° and a K of 37. The obtained discontinuity sets show good agreement with those previously mapped by Monsalve et al. in an area adjacent to the same case study mine [20]. This indicates that both study sections present similar structural domains. The presence of some random discontinuities showing on the stereo net could be attributed to the presence of fractures associated to the blasting process. As it was previously described, it is possible to observe on the field radial fracturing patterns close to the blast hole indicating damage on the rock mass due to the explosive damage.

Once the discontinuity sets were defined and the six subsampled datasets were generated, the PDF fitting and PDF comparison steps for the desired parameters was conducted. Figure 9 summarizes the results from these two steps with regard to discontinuity trace length. On the top of the figure, one can observe the comparison between the PDFs obtained from both mapping methods for each discontinuity set. The mapping windows beneath each of the PDFs correlates to their respective discontinuity set, showing the automatically extracted discontinuities in blue and the manually mapped fractures in green. It is possible to observe for each of the three discontinuity sets that the distribution parameters for both I-Site and DSE-extracted discontinuities have a log-normal distribution. In all three cases, the distribution obtained from DSE looks more skewed to the left, indicating that the ADES depicted smaller-sized discontinuities, as mentioned before. This can also be visually evidenced in the mapping windows where some discontinuities seem to be mapped exactly the same from both methods, while smaller fractures were mapped in blue. These results were also statistically supported by the previously mentioned hypothesis tests, indicated in Table 1. For the three discontinuity sets, results indicated that the mean trace length values were significantly different

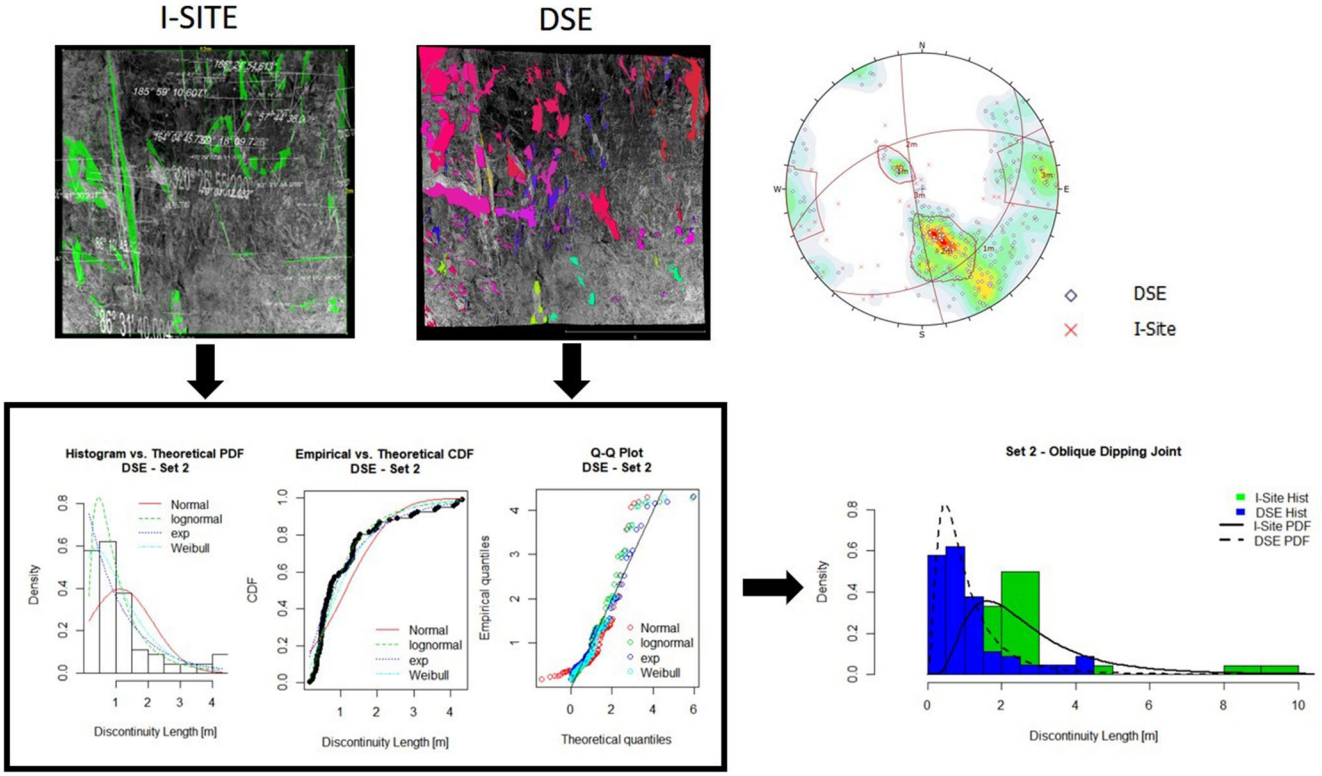

Fig. 5 Data analysis process flowchart

between the I-Site and DSE-extracted discontinuities. However, trace length variances were statistically similar for both methods in all discontinuity sets.

Furthermore, the discontinuity spacing analysis yielded results indicating that spacings measured from the DSE-extracted discontinuities were similar to those measured

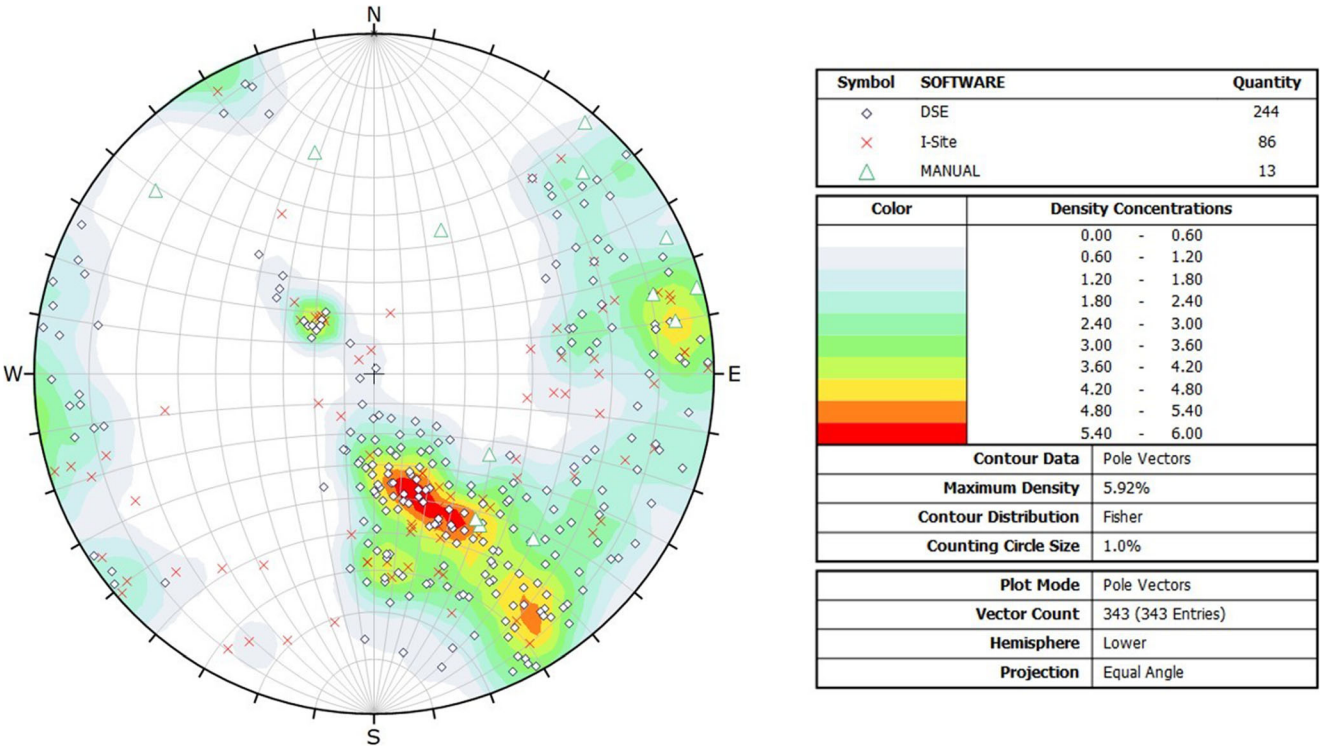

Fig. 6 Overall stereographic analysis comparing discontinuities mapped from DSE, I-Site, and manually on the field

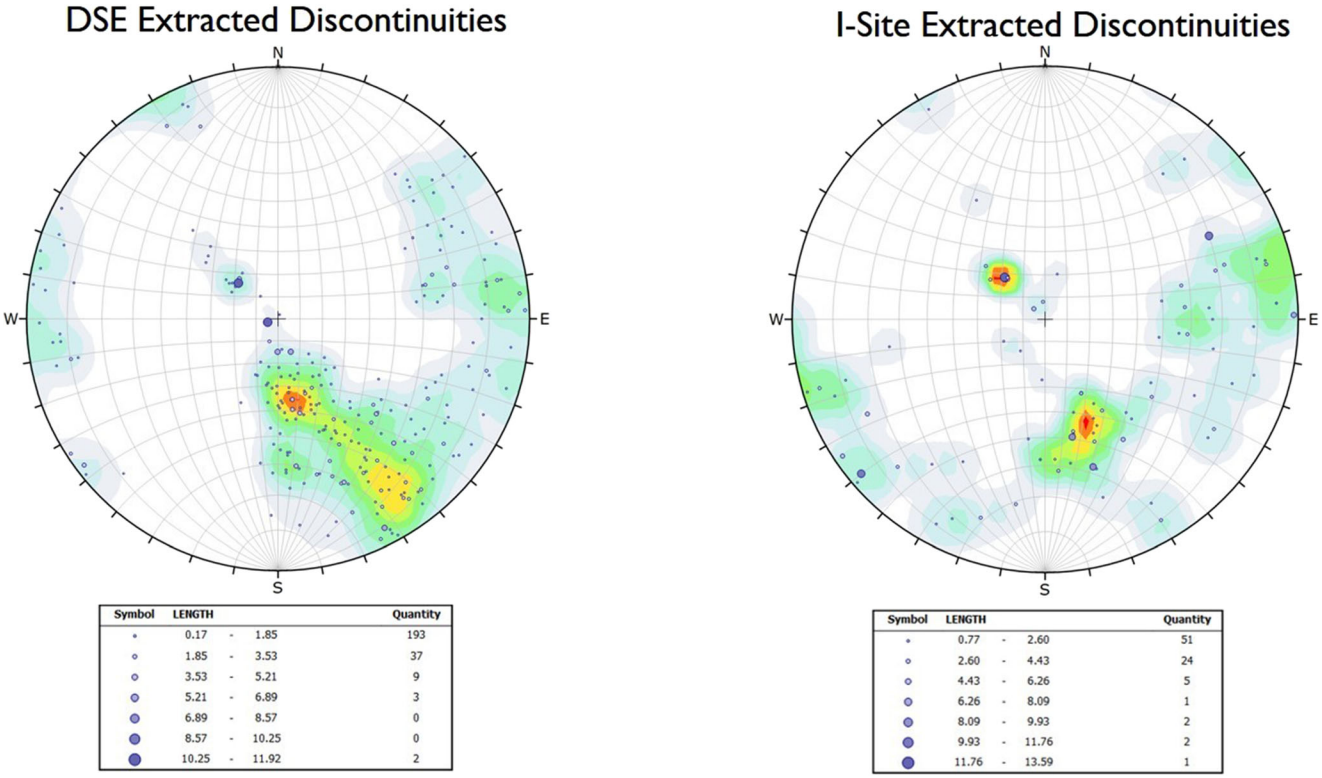

Fig. 7 Comparison between DSE extracted and I-Site extracted discontinuities by discontinuity trace length

within I-Site. Figure 10 indicates the spacing PDFs and visually depicts these values. In the three cases, the DSE obtained PDFs seem to be closer to the ones obtained from I-Site. This is validated by the statistical results provided in Table 1, indicating that for sets 1 and 2, the spacing measurements obtained from DSE are statistically the same as the ones obtained from I-Site. Set 3 results indicated that DSE extracted discontinuities did not present the same spacing distribution as the ones extracted from I-Site.

With regard to the processing time comparison between both mapping methods, Table 2 summarizes the results. On average, a discontinuity can be mapped on I-Site in 48 s. Therefore, the amount of time to map a point cloud section will depend on the size of the point cloud and the amount of

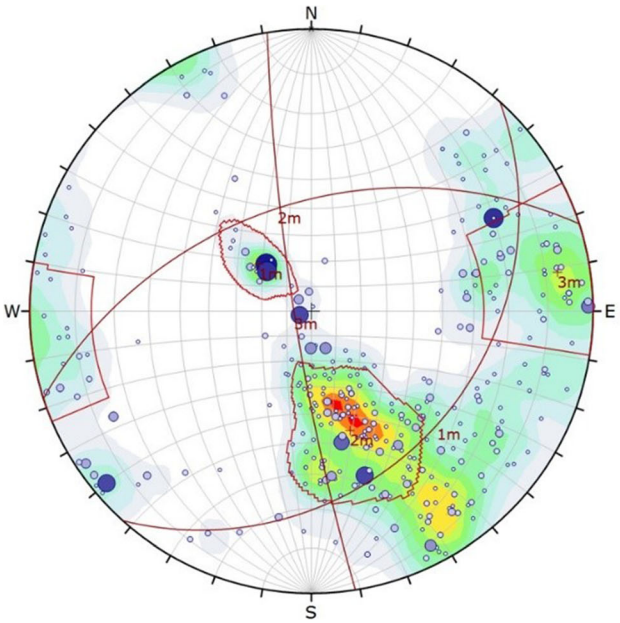

Symbol	LENGTH		Quantity
	0.17	1.51	205
	1.51	2.85	76
	2.85	4.20	31
	4.20	5.54	6
	5.54	6.88	4
	6.88	8.22	1
	8.22	9.56	1
	9.56	10.90	3
	10.90	12.25	2
	12.25	13.59	1

Set	Dip	Dip Direction	Fisher K	Label
1	27.88	132.34	118.72	Bedding Plane
2	47.74	342.26	24.07	Oblique Dipping Joint
3	83.43	261.30	37.80	Vertical Parallel to Dip Joint

Fig. 8 Main discontinuity set definition

Table 1 Summary of statistical tests for variance and mean of spacing and joint trace length obtained from DSE and I-Site extracted discontinuities

Parameter/SET		Software	Distribution	Mean	Standard deviation	Number of mapped fractures	Variance comparison		Mean comparison	
							F test	*p* value	*t* test	*p* value
Trace length	1	I-Site	Log-normal	1.236	0.7	8	0.650	0.584	2.328	0.032
		DSE	Log-normal	0.359	0.889	12				
	2	I-Site	Log-normal	0.82	0.584	24	0.593	0.155	6.821	1.71E-08
		DSE	Log-normal	0.179	0.769	90				
	3	I-Site	Log-normal	0.841	0.481	15	1.129	0.745	4.098	3.60E-04
		DSE	Log-normal	0.214	0.462	32				
Spacing	1	I-Site	Normal	2.073	0.461	5	0.896	0.988	1.252	0.248
		DSE	Normal	1.732	0.523	14				
	2	I-Site	Log-normal	0.327	0.285	30	1.195	0.495	1.814	0.077
		DSE	Log-normal	0.221	0.264	128				
	3	I-Site	Normal	2.600	0.649	14	1.298	0.511	3.289	0.003
		DSE	Normal	1.933	0.584	40				

discontinuities present. On the contrary, DSE processing time depends on the size and density of the point cloud, rather than the amount of discontinuities mapped. On average, it took 3.75 h longer to process the point clouds on DSE than directly manually mapping the discontinuities on I-Site. However, the processing for automatically generating the discontinuities does not include the processing time to convert this point clouds into faces with Cloud Compare.

Today, international ground control best practices indicate that ground control management plans (GCMP) are one of the most effective tools to forecast and prevent ground control related risks [26, 27]. A GCMP is a multilevel dynamic document grounded in modern risk management tailored to managing all ground control related issues in an underground mine operation. Among some of the elements composing a GCMP are included geotechnical characterization, ground control hazard recognition, and ground inspection and monitoring [28]. As remote sensing techniques become cost-effective and accessible to mining operators, and automated discontinuity mapping algorithms continue to evolve, the application of these technologies provides engineers with tools to forecast and control ground control related risks. Results from these mapping processes not only are useful for identifying fractures and discontinuities prone to produce a rock fall condition but also can be integrated to advanced numerical modeling, and probabilistic risk analysis design approaches [4, 29].

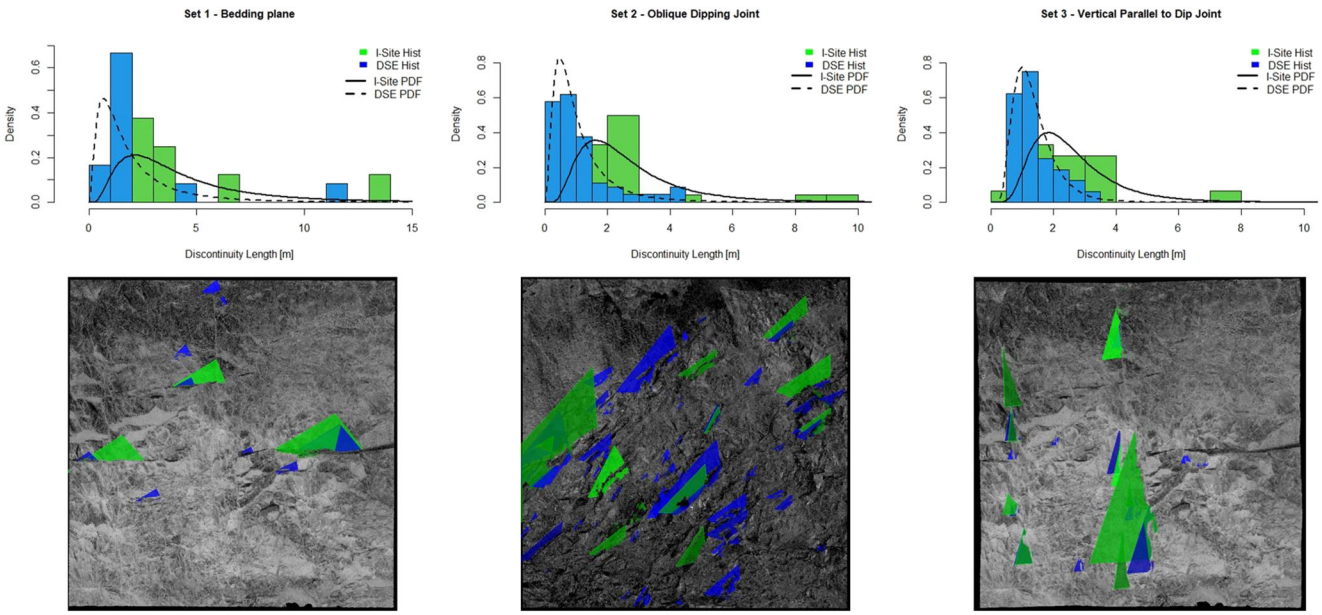

Fig. 9 Statistical Summary of comparison between trace length of discontinuity sets obtained with DSE and I-Site

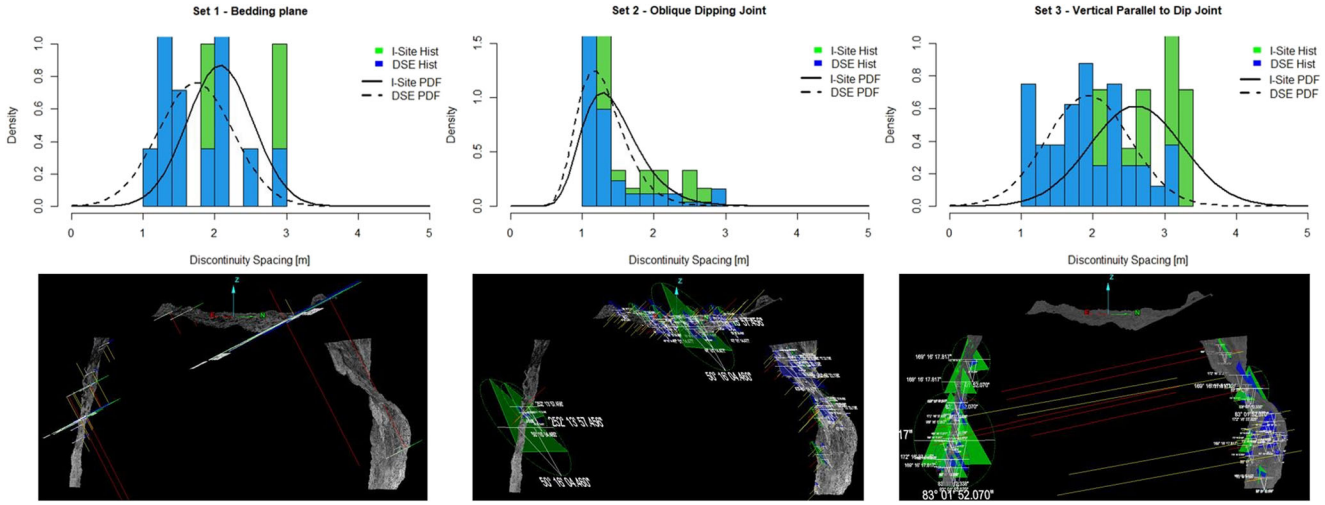

Fig. 10 Statistical summary of comparison between spacing of discontinuity sets obtained with DSE and I-Site

7 Conclusions

This paper has introduced two alternative methods for rock mass characterization that are different from conventional discontinuity mapping: manual virtual discontinuity mapping (MVDM) and automated discontinuity extraction software (ADES). Both methods work on point clouds extracted from conventional remote sensing techniques such as laser scanning and photogrammetry. In this work, both methods were used to map discontinuities on three predefined 144 m^2 mapping windows. Manual and automatically extracted discontinuities were used to define the main discontinuity sets within the areas of interest. Three main discontinuity sets were defined, and their orientations and statistical distribution properties were estimated for each by performing a stereographic analysis. After the definition of the three discontinuity families, a statistical analysis was performed to compare the trace length and spacing probability distributions for each set from each mapping method. Results from these PDF estimations were used to evaluate the performance of the automated extraction software. The following are conclusions derived from this work:

- MVDM and ADES were successfully compared under controlled conditions. Results indicated that ADE yielded results that could be comparable with the manually mapped discontinuities.
- Three main discontinuity sets were defined as a result of the mapping process. The same discontinuity sets were identified by the two compared methods.
- The parameters used to compare both mapping processes were number of extracted discontinuities, orientation, trace length, spacing, and processing time.
- Resulting mapped discontinuities were compared by statistical inference procedures. In addition to that a visual inspection of the mapping results allowed us to understand the statistical results.
- ADES identifies and maps smaller discontinuities that may not be mapped by the user in MVDM based on its engineering judgment (smaller discontinuities may not have a severe impact on the stability of the excavation).
- DSE is an open source software, and its results indicate that it could be successfully used and implemented by mining operators to gain insight into the structural condition of the mine operation and ultimately identify potential rock fall hazards.
- Even though DSE requires more processing time than MVDM, it allows engineers to allocate this time to other tasks.
- Even though, ADES can extract the discontinuities automatically, additional supervision by the engineer is required to avoid the extraction of planes that do not correspond to real geological structures in the field. Filtering the results from the

Table 2 Processing time comparison between ADES and MVDM

Section	Number of points	I-Site		DSE		Difference (h)
		Number of discontinuities	Mapping time (h)	Number of discontinuities	Mapping time (h)	
Rib	4,671,120	36	0.48	109	1.98	1.5
Roof	5,076,309	27	0.36	80	2.3	1.94
Karst	1,695,942	23	0.31	55	0.62	0.31
Total	11,443,371	86	1.15	244	4.9	3.75

automated mapping is important to avoid misleading information.

Acknowledgements The authors would like to thank Lhoist mining engineers and management for their support and guidance during this project. MAPTEK is acknowledged for providing a license of the software I-Site Studio.

Funding This work is funded by the NIOSH Mining Program under Contract No. 200-2016-91300. Views expressed here are those of the authors and do not necessarily represent those of any funding source.

Declarations

Conflict of Interest The authors declare that they have no conflict of interest.

References

1. MSHA (2020) "Accident Injuries Data Set," Mine Safety and Health Administration
2. Esterhuizen GS, Dolinar DR, Ellenberger JL, Prosser LJ (2011) Pillar and Roof Span Design Guidelines for Underground Stone Mines. National Institute for Occupational Safety and Health, Pittsburg
3. Brown E (2012) Risk assessment and management in underground rock engineering - an overview. J Rock Mech Geotech Eng 4:193–204
4. Joughin W, Muaka J, Mpunzi P, Sewnun D, Wesseloo J (2016) "A risk-based approach to ground support design," in Ground Support 2016, Lulea
5. Barton N (1978) Suggested methods for the quantitative description of discontinuities in rock masses. Int J Rock Mech Min Sci Geomech 15(6):319–368
6. Chao J, Yong L, Mingyuan L, Xiaoyong Z (2017) Jointed surrounding rock mass stability analysis on an underground cavern in a hydropower station based on the extended key block theory. Energies 10(4):563
7. Monsalve J, Baggett J, Soni A, Ripepi N, Hazzard J (2019) Stability analysis of an underground limestone mine using terrestrial laser scanning with stochastic discrete element modeling. 53rd US Rock Mechanics/Geomechanics ARMA Symposium, New York
8. Grenon M, Landry A, Hadjigeorgiou, Lajoie, P (2017) Discrete fracture network based drift stability at the Éléonore Mine. Mining Technol 126(1):22–33
9. Fu G, Ma G, Qu X, Huang D (2016) Stochastic analysis of progressive failure of fractured rock masses containing non-persistent joint sets using key block analysis. Tunn Undergr Space Technol 51:258–269
10. Jing L, Stephansson O (2007) Discrete Fracture Network (DFN) Method. In: Fundamentals of Discrete Element Methods for Rock Engineering Theory and Applications. ELSEVIER, Amsterdam, pp 365–398
11. Voyay I, Roncella R, Forlani G, Ferrero A (2006) Advanced techniques for geo structural surveys in modelling fractured rock masses: application to two Alpine sites. Laser Photogramm Methods Rock Face Charact:102–108
12. Cacciari P, Futai M (2015) "Mapping and characterization of rock discontinuities in a tunnel using 3D terrestrial laser scanning," Bull Eng Geol Environ
13. Rogers S, Bewick R, Brzovic A, Gaudreau D (2017) "Integrating photogrametry and discrete fracture network modelling for improved conditional simulation of underground wedge stability," 8th International Conference in Deep and High Stress Mining, pp. 599-610
14. Riquelme A, Abellan A, Tomás R, Jaboyedoff M (2014) A new approach for semi-automatic rock mass joints recognition. Comput Geosci 68:38–52
15. Dewez T, Girardeau-Montaut D, Allainc C, Rohmer J (2016) "FACETS: A Cloud Compare plugin to extract geological planes from unstructured 3D point clouds," in Int. Arch. Photogramm. Remote Sens. Spatial Inf. Sci., Prage
16. Kemeny J, Donovan J (2005) "Rock mass characterisation using LiDAR and automated point cloud processing," Min Geol Eng 38(11):26–29
17. Zhang P, Li J, Yang X, Zhu H (2018) Semi-automatic extraction of rock discontinuities from point clouds using the ISODATA clustering algorithm and deviation from mean elevation. Int J Rock Mech Min Sci 110:76–87
18. Zhang P, Du K, Tannant D, Zhu H, Zheng W (2018) Automated method for extracting and analysing the rock discontinuities from point clouds based on digital surface model of rock mass. Eng Geol 239:109–118
19. Guo J, Liu Y, Wu L, Liu S, Yang T, Zhu W, Zhang Z (2019) A geometry- and tecture-based automatic discontinuity trace extraction method for rock mass point cloud. Int J Rock Mech Min Sci 124(104132):1–10
20. Monsalve J, Baggett J, Bishop R, Ripepi N (2019) Application of Laser Scanning for Rock Mass Characterization and Discrete Fracture Network Generation in an Underground Limestone Mine. Int J Min Sci Technol 29:131–137
21. Esposito G, Mastrorocco G, Salvini R, Oliveti M, Starita P (2017) "Application of UAV photogrammetry for the multi-temporal estimation of surface extent and volumetric excavation in the Sa Pigada Bianca open-pit mine, Sardinia, Italy," Environ Earth Sci volume 76
22. Slaker B (2015) Monitoring underground mine displacement using photogrammetry and laser scanning. Virginia Tech, Blacksburg
23. Gabara G, Sawicki P (2017) A new approach for inspection of selected geometric parameters of a railway track using image-based point clouds. Sensors 18(3):791
24. Rocscience, "Rocsicence," 26 August 2019. [Online]. Available: https://www.rocscience.com/help/dips/#t=dips%2FGetting_Started.htm. Accessed 26 August 2019
25. Vose D (2008) Risk analysis: a quantitative guide. John Wiley & Sons
26. Emery J, Canbulat I, Zhang C (2020) Fundamentals of modern ground control management in Australian underground coal mines. Int J Min Sci Technol 30:573–582
27. Hawley M, Marisett S, Beale G, Stacey P (2009) Performance assessment and monitoring. In: Guidelines for Open Pit Slope Design. CSIRO, Collingwood, pp 327–380
28. Department of Mines, Industry Regulation and Safety, "Ground control management in Western Australian mining operations - guideline," Department of Mines Industry Regulations and Safety, Western Australia, 2019
29. Monsalve J, Soni A, Rodriguez-Marek A, Ripepi N (2020) "A preliminary investigation on stochastic discrete element modeling for pillar strength determination in underground limestone mines from a probabilistic risk analysis approach," in 39th International Conference on Ground Control in Mining